Strain-tunable silicon photonic band gap microcavities in optical waveguides

Chee Wei Wong[a)]
Department of Mechanical Engineering, Massachusetts Institute of Technology, Cambridge, Massachusetts 02139

Peter T. Rakich and Steven G. Johnson
Department of Physics, Massachusetts Institute of Technology, Cambridge, Massachusetts 02139

Minghao Qi and Henry I. Smith
Department of Electrical Engineering and Computer Science, Massachusetts Institute of Technology, Cambridge, Massachusetts 02139

Erich P. Ippen
Department of Physics and Department of Electrical Engineering and Computer Science, Massachusetts Institute of Technology, Cambridge, Massachusetts 02139

Lionel C. Kimerling
Department of Materials Science and Engineering, Massachusetts Institute of Technology, Cambridge, Massachusetts 02139

Yongbae Jeon, George Barbastathis, and Sang-Gook Kim
Department of Mechanical Engineering, Massachusetts Institute of Technology, Cambridge, Massachusetts 02139

(Received 20 October 2003; accepted 19 December 2003; publisher error corrected 8 March 2004)

We report the design, device fabrication, and measurements of tunable silicon photonic band gap microcavities in optical waveguides, using direct application of piezoelectric-induced strain to the photonic crystal. We show, through first-order perturbation computations and experimental measurements, a 1.54 nm shift in cavity resonances at 1.56 μm wavelengths for an applied strain of 0.04%. The strain is applied through integrated piezoelectric microactuators. For operation at infrared wavelengths, we combine x-ray and electron-beam lithography with thin-film piezoelectric processing. This level of integration permits realizable silicon-based photonic chip devices, such as high-density optical filters, with active reconfiguration. [DOI: 10.1063/1.1649803]

Real-time reconfigurability is desirable for photonic crystal based telecommunication devices, as a means of provisioning optical networks and compensating for performance variations due to tight manufacturing tolerances or external disturbances. To this end, the modulation of photonic crystal optical properties through application of small strain was recently proposed.[1] Permanent deformations on the photonic crystal unit cell or defects have also been investigated for control of polarization,[2] coupled resonators field distributions,[3] and quality factors in microcavity lasers.[4]

Here we demonstrate the design and experimental observations of tunable microcavity resonances through direct application of strain from integrated piezoelectric microactuators. The conceptual design of the strain-tunable platform is illustrated in Fig. 1. Four piezoelectric microactuators, each consisting of a tri-layer of platinum (Pt) top electrode, a lead zirconate titanate (PZT), and a Pt bottom electrode, are anchored onto the SiO_2 deformable membrane. An optical waveguide with a photonic band gap microcavity[5] is located on the membrane between the microactuators. Active strain from the PZT microactuators, when placed under differential applied voltages, results in plane-strain deformation of the membrane and, hence, strain-induced perturbation of the microcavity. Compared with electro-optic[6,7] methods, piezoelectric strain-tuning is more practical toward silicon-based integrated photonic systems, given the weak Kerr nonlinearities in silicon. Moreover, compared with thermal[8,9] methods, piezoelectric strain-induced tuning permits nanowatt power consumption per active device as opposed to milliwatts, microsecond response times as opposed to milliseconds, and spatially localized tunability for high-density integration. With the small-strain perturbation, order of 0.1%, the proposed device is expected to achieve at least greater than 10^9 repeated cycles, as performed on related deformable membranes,[10] without observable mechanical fatigue.

As shown in Fig. 2(a), the microcavity is formed by the introduction of a point defect into a periodic array of holes in the high-index contrast Si waveguide. The waveguide has submicrometer dimensions ($t=176$ nm and $w=541$ nm), is single-mode, and sits on a low-index SiO_2 ridge ($t_{ox}=296$ nm). The periodic structure, with lattice constant a, splits the lower order guided mode to form a photonic band gap. The introduction of a defect—by adding dielectric material between two holes at the center of the periodic structure—permits a spatially localized resonant state to exist

[a)]Electronic mail: cheewei@alum.mit.edu

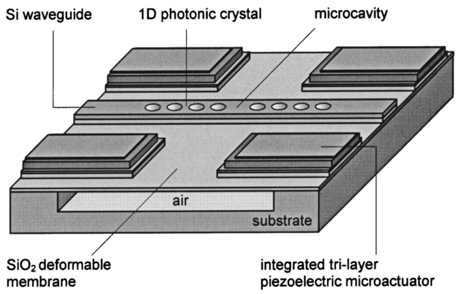

FIG. 1. Cross-section schematic of the strain-tunable microcavity (not drawn-to-scale). The microcavity employs a one-dimensional photonic crystal to confine light along the direction of the submicron optical waveguide, and total internal reflection for confinement in the transverse direction. Each piezoelectric microactuator has 233 μm active length, 23 μm width, and 0.3 μm thickness.

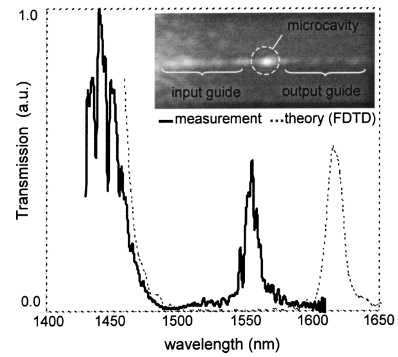

FIG. 3. Measured transmissions of the microcavity, depicting the band edge and resonance at 1555.2 nm with a Q of 159 ± 10. The dotted lines depicted FDTD calculations, based on measured device dimensions. The superimposed shorter wavelength modulations on the transmission are from electron-beam stitching errors in the waveguide fabrication. Inset: imaged top view of microcavity with guidance in the waveguides.

in the band gap. The design has dimensions $a=429$ nm, $a_d=643$ nm, and $d=189$ nm. The electric field distribution is found through three-dimensional (3D) finite-difference time-domain (FDTD) computations. Figure 2(b) shows the electromagnetic energy distribution sliced through the middle of the microcavity. The observed strong field confinement gives a modal volume of 0.055 μm^3, about $5(\lambda/2n)^3$, where λ is the resonant wavelength and n the silicon refractive index. The microcavity quality factor Q, defined as $\lambda/\delta\lambda$ where $\delta\lambda$ is the full-width half-maximum of the microcavity transmission, is estimated to be 175. Applications of the microcavity include high-density optical filters and spontaneous-emission enhancement devices.

To study the effects of small strain (order 0.1% or less) on the microcavity, we employ first-order perturbation theory[11] to obtain a semianalytical result for the strain-induced shift $\Delta\lambda$ in the resonant wavelength of the microcavity. First, the results of the 3D FDTD calculation are linearly interpolated to obtain the fields at the dielectric interfaces. Next, a closed-form solution for the elliptical displacements of the dielectric interfaces is derived from classical mechanics.[12] The applied stresses are assumed to be free from discontinuities and the strain components are solved in polar coordinates with appropriate boundary conditions to obtain analytical expressions of the hole elliptical displacements. These displacements and the relevant FDTD fields are utilized to compute well-defined surface integrals of the unperturbed fields over the perturbed interface, as described by the perturbation theory. The results are repeated for various applied stress perturbations $\Delta\sigma$ to determine the corresponding resonance shifts $\Delta\lambda$. For example, for a 0.05% strain, $\Delta\lambda$ is predicted to be 2.1 nm (normalized for operation at 1.55 μm wavelengths) from a full 3D computation. While there are three components—hole ellipticity, defect length a_d, and lattice constant a—in the strain perturbation, the major contribution is determined to be from changes in the defect length. A two-dimensional (2D) computation gives a similar final result for $\Delta\lambda$, although the various contributions differ from the more accurate 3D computation. Other effects such as index change due to applied stresses are found to be secondary, changing $\Delta\lambda$ by less than 1% fractional difference, for a strain of 0.1%.

Fabrication of the device necessitates the combination of x-ray and electron-beam lithography with thin-film piezoelectric microfabrication. X-ray lithography, with a Cu_L source at 1.3 nm, is used with a mask fabricated using electron-beam lithography to obtain 130 nm minimum feature sizes for operation at 1.55 μm wavelengths. A scanning electron micrograph of the fabricated microcavity is illustrated in Fig. 2(a). The fabricated thin-film microactuators have a piezoelectric dielectric constant of 1200 and a piezoelectric coefficient d_{31} about -100 pC/N. The completed chip, before packaged for testing, is shown in Fig. 2(c).

To test the microcavities, two tunable laser diodes are used to provide a measurement window from 1430 to 1610 nm. A polarization controller and a fiber-coupled lens assembly were used to couple light into the structure. The resulting waveguide mode was imaged onto a photodetector and the signal was processed with a lock-in amplifier. The inset of Fig. 3 shows the top view of the coupled waveguides and the microcavity, captured with infrared cameras. Waveguide transmission losses were investigated through the Fabry–Perot resonance methodology[13] using the cleaved facets of waveguides in devices without microcavities, and were determined to be between 5 and 7 dB/cm.

The measured microcavity transmission spectrum, with-

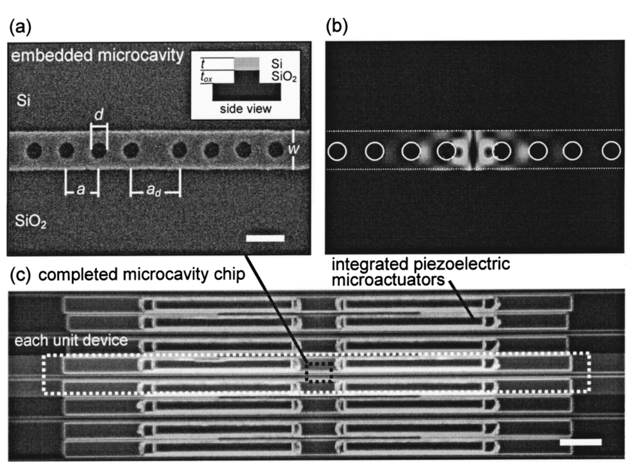

FIG. 2. Images of completed microcavity chip and numerical experiments on the field distribution. (a) Scanning electron micrograph of the embedded microcavity patterned by x-ray lithography. Inset: side-view of Si waveguide on SiO_2 ridge. Scale bar: 500 nm. (b) Electric energy distribution at middle 2D slice of microcavity, at resonance. (c) Top view of completed strain-tunable microcavity with integrated piezoelectric microactuators. Scale bar: 100 μm.

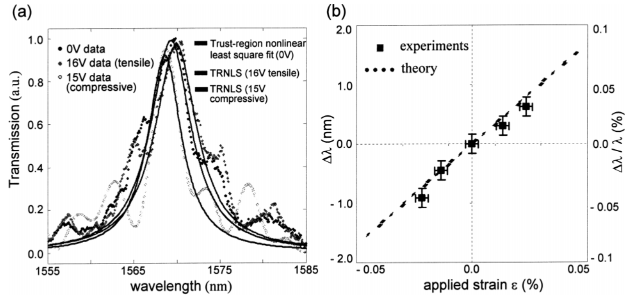

FIG. 4. Measurements and analysis of strain-tuned microcavity resonances. (a) Measured dynamic tuning of microcavity resonances under different dc-biased applied voltages, for tensile and compressive stresses to the microcavity. The shifts in resonance for each applied voltage are averaged over multiple measurements for each value of voltage. The variance in resonant wavelength, without any active tuning, is determined to be 0.02 nm from multiple measurements. (b) Comparison of strain-tuned experiments with first-order perturbation computations. The vertical error bars (± 0.17 nm) are from variations on the nonlinear least squares fitting algorithm; the horizontal error bars (2.7×10^{-3}%) are uncertainties in the Computer Microvision displacement measurements.

out active strain, is shown in Fig. 3. The higher-frequency band edge is at approximately 1450 nm, with excellent matching between experiment and theory without any fitted parameters. The microcavity resonance is observed at 1555.2 nm, with the FDTD predictions deviating by a 3.8% fractional difference. Although this represents a 59.3 nm deviation, the percentage deviation is well within the numerical resolution of the FDTD and the measurement accuracy of the device dimensions. The measured Q is 159, below the FDTD predictions of 175. This discrepancy is likely due to residual fabrication imperfections leading to increase in cavity losses. It should be possible to significantly increase Q to well over 10^3 by well-known techniques, such as a small increase in the modal volume or a forced cancellation of the lowest order multipole term in the far-field radiation field.[14]

When a dc bias is applied to the piezoelectric microactuators, the maximum $\Delta\lambda$ is determined to be $+0.63$ nm for 16 V (tensile stress) applied and -0.91 nm for 15 V (compressive stress) applied. The tension and compression stresses are possible based on the location of the microcavity and the specific set of microactuators activated. Figure 4(a) shows the strain-tuned resonances for the various applied voltages. The fitted Lorentzians are generated through a trust-region nonlinear least squares algorithm[15] with R^2 values of 0.94 ± 0.03. For the particular dimensions of the microcavity, Q degrades by about 3% when under tension and improves when under compression. This is due to the dependence of Q on the field profile and position[14] in the band gap, both of which change under the applied strain.

Figure 4(b) compares the measurements with the first-order perturbation predictions. The applied strain is estimated through Computer Microvision, an instrument that can measure displacement with nanometer precision.[16] The results are in excellent agreement: for an applied strain of 0.04%, first-order perturbation theory predicts a $\Delta\lambda$ of 1.55 nm while our experimental measurements show a $\Delta\lambda$ of 1.54 ± 0.17 nm. We expect, however, larger deviations for larger applied strains, since our predictions capture only the first-order perturbation.[17]

In summary, we investigated the real-time configurability of silicon photonic band gap microcavities in optical waveguides, using direct application of piezoelectric induced strain. The tuning of the cavity resonance was first predicted theoretically through first-order perturbation theory on FDTD computations. By combining x-ray lithography, electron-beam lithography, and thin-film piezoelectric microfabrication, we built the tunable microcavities for operation at 1.55 μm. Experimental measurements demonstrate the cavity resonance shifts, within the band gap, when a strain is applied through the integrated microactuators, in agreement with our predictions. The results and analysis presented in this letter provide confidence that dynamic strain-tuning of photonic crystal devices is a realizable step toward practical photonic crystal implementations. Possible applications include postfabrication trimming for passive silicon-based integrated photonic systems, active feedback compensation for external disturbances, and device reconfiguration toward tunable optical filters. For the latter, a larger tuning range would be required, and it is possible for up to 8 nm (0.2% strain) at 1.55 μm optical wavelengths. This would be accomplished by delivering a larger force to the microcavity via a reduction in the membrane residual stress, wherein most of the elastic energy is dissipated, or in the membrane thickness.[18]

The authors thank Salil Desai, Juan Ferrara, Jeffrey T. Hastings, James M. Daley, and Dennis M. Freeman for their invaluable assistance. The work is supported by the Microphotonics Center and the Department of Mechanical Engineering at the Massachusetts Institute of Technology.

[1] S. W. Kim and V. Gopalan, Appl. Phys. Lett. **78**, 3015 (2001).
[2] S. Noda, M. Yokoyama, M. Imada, A. Chutinan, and M. Mochizuki, Science **293**, 1123 (2001).
[3] H. Pier, E. Kapon, and M. Moser, Nature (London) **407**, 880 (2000).
[4] J. Vuckovic, M. Loncar, H. Mabuchi, and A. Scherer, Phys. Rev. E **65**, 016608 (2001).
[5] J. S. Foresi, P. R. Villeneuve, J. Ferrera, E. R. Thoen, G. Steinmeyer, S. Fan, J. D. Joannopoulos, L. C. Kimerling, H. I. Smith, and E. P. Ippen, Nature (London) **390**, 143 (1997).
[6] P. Halevi and F. Ramos-Mendieta, Phys. Rev. Lett. **85**, 1875 (2000).
[7] K. Yoshino, Y. Shimoda, Y. Kawagishi, K. Nakayama, and M. Ozaki, Appl. Phys. Lett. **75**, 932 (1999).
[8] A. Figotin, Y. A. Godin, and I. Vitebsky, Phys. Rev. B **57**, 2841 (1998).
[9] K. Busch and S. John, Phys. Rev. Lett. **83**, 967 (1999).
[10] C. W. Wong, Y.-B. Jeon, G. Barbastathis, and S.-G. Kim, Appl. Opt. **42**, 621 (2003).
[11] S. G. Johnson, M. Ibanescu, M. A. Skorobogatiy, O. Weisberg, J. D. Joannopoulos, and Y. Fink, Phys. Rev. E **65**, 066611 (2002).
[12] S. P. Timoshenko and J. N. Goodier, *Theory of Elasticity*, 2nd ed. (McGraw–Hill, New York, 1970).
[13] R. Regener and W. Sohler, Appl. Phys. B: Photophys. Laser Chem. **36**, 143 (1985).
[14] S. G. Johnson and J. D. Joannopoulos, *Photonic Crystals: The Road from Theory to Practice*, 1st ed. (Kluwer Academic, Norwell, 2002).
[15] M. A. Branch, T. F. Coleman, and Y. Li, SIAM J. Sci. Comput. (USA) **21**, 1 (1999).
[16] D. M. Freeman, A. J. Aranyosi, M. J. Gordon, and S. S. Hong, Technical Digest of Solid-State Sensor and Actuator Workshop, Transducers Research Foundation, Cleveland Heights, OH, 1998, p. 150.
[17] Higher-order perturbations suffer from the incomplete basis of our eigenproblem in terms of the electric field. However, we could cast the eigenproblem in terms of the magnetic field (such that $\nabla\cdot\mu\mathbf{H}=0$ is satisfied) to compute higher-order corrections. Issues of fast-convergence, however, would need to be solved.
[18] A variational approach to the elastic strain energy in the double-anchored membrane suggests residual stress is the largest contributor, following the technique shown by Senturia, S. D., *Microsystem Design* (Kluwer Academic Publishers, Massachusetts, 2001).